

Restricted BPA: Applying Ball-Pivoting on the Plane

Esdras Medeiros¹, Luiz Velho¹ and H elio Lopes²

¹IMPA–Instituto de Matem atica Pura e Aplicada,
{esdras, lvelho}@visgraf.impa.br

²PUC–Pontif icia Universidade Cat olica do Rio de Janeiro,
lopes@mat.puc-rio.br

Abstract

In this article we propose a new 2D triangulation method based on the ball-pivoting algorithm (BPA). The BPA is an interesting advancing front approach for surface reconstruction that uses a ball of fixed radius traversing the 3D sample points by pivoting front edges and attaching triangles to the mesh. Given a set of 2D points, our method applies the BPA on them assuming that they have a constant third coordinate. We show that such geometrical restriction implies in several simplifications on the original BPA implementation. We demonstrate that the resulted triangulation is a solid alpha complex, a special subset of Delaunay Triangulations that is closely related to alpha shapes. The BPA efficiency is extremely dependent on the uniformity of the sampling and on the ball radius. We also present an efficient generalization of our method to obtain, in an adaptive way, 2D solid alpha complexes of generic samplings (uniform or non-uniform) free from the influence of ball size.

1. Introduction

During the last two decades the problem of triangulating a set of points in \mathbb{R}^n , specially for $n = 2$, has been thoroughly investigated in many domains, including imaging computer vision, terrain modeling and meshing for solving PDE. Despite of many solutions for this problem can be found, Delaunay triangulations (DT) along with its dual, the Voronoi Diagram, has received a great attention by the research community. Its success on uncountable applications comes from some nice features it contains, namely the maximization of the smallest angle (only in the 2D case) and the in-circle property (no point in the point set falls in the circumcircle of any triangle in the triangulation). In the literature, one can find many DT algorithms, some of which are surveyed and evaluated by Fortune [8] and Su and Drysdale [13].

As a subset of DT we outstand the *alpha complexes* and the *alpha shapes* [7, 6] families. Both are important tools for shape recognition of a set of points. Each alpha complex is a well defined simplicial complex parameterized by a real number α which describes its level of “detail”. An alpha shape is the underlying polyhedron of an alpha complex.

In 3D Photography context [4], we encounter an algorithm for surface reconstruction that is closely associated with the alpha shape: the *ball-pivoting algorithm* (BPA)[3]. It is an interesting advancing front approach [10, 9] for surface interpolation that uses a ball of fixed radius traversing the sample points by pivoting front edges of a current active boundary and creating elements (triangles) that are attached to the mesh.

Contributions. The first contribution of this paper is the introduction of the *solid alpha-complexes* concept. Our final aim is to present a new triangulation algorithm of 2D data points based on the ball-pivoting. Given a set of 2D points, our method applies the BPA on them assuming that they have a third constant coordinate. Because of such geometric constraint, we named it Restricted Ball-Pivoting Algorithm (RBPA). Our implementation has a number of features and contributions:

- It is a direct method for the construction of 2D *solid alpha complex*, which is a subset of an alpha-complex (see section 2.4), without computing DT.
- It simplifies the BPA data structure and geometric computations taking advantage of the fact that all points are at a common plane.
- It exhibits linear time complexity for uniform distributed points. No data sorting is required.
- It is generalized to obtain, in an adaptive way, 2D solid alpha complexes of generic samplings (uniform or non-uniform) free from the influence of ball size.

Overview. The outline of this paper is as follows. In the next section we review basic concepts on simplicial complexes, Delaunay triangulations, alpha complexes and alpha shapes families and introduce the *solid alpha complex* concept. In section 3 we firstly describe the BPA including its geometric step, mesh construction and data structure. After that we introduce our method: the RBPA. We show in section 4 the relation between 2D solid alpha complexes and the output of RBPA. In section 5 we analyse RBPA behavior on uniform samplings regarding its efficiency for different ball sizes. In section 6 we present a hierarchical generalization of the RBPA for generic samplings and analyse its complexity. In section 7 we show some examples and applications. Finally section 8 concludes this article proposing future extensions and improvements.

2. Basic Concepts

One objective of this section is to describe several concepts in topology and in computational geometry that will be used in this work. Other important objective is to introduce the concept of *solid alpha complex*.

2.1. Simplicial Complexes

A k -simplex $\sigma_T = \text{conv}(T)$ is the convex combination of an affinely independent point set $T \subset \mathbb{R}^n$, $\#T = k + 1$; $0 \leq k \leq n$; and $\#$ denotes the cardinality. k is the dimension of the simplex σ_T . A *simplicial complex* K is a finite collection of simplices with the following two properties:

1. if $\sigma_T \in K$ then $\sigma_U \in K$, $U \subset T$.
2. if $\sigma_U, \sigma_V \in K$, then $\sigma_{T \cap V} = \sigma_U \cap \sigma_V$.

Both properties above imply that $\sigma_{T \cap V} \in K$. The underlying polyhedron of K is $|K| = \cup_{\sigma \in K} \sigma$. A subcomplex L of K is a simplicial complex $L \subset K$.

An α -ball b is an open ball with radius α . We say that the α -ball b is empty if $b \cap S = \emptyset$. A k -simplex σ_T , $0 \leq k \leq n - 1$ is α -exposed if there exists an empty α -ball b such that $T = \partial b \cap S$.

Based on this simplicial structure we will define some simplicial artefacts such as Delaunay Triangulations, alpha complexes and alpha shapes.

2.2. Delaunay Triangulations

The Delaunay triangulation of a set of points on the plane is a unique set of triangles connecting the points satisfying an “empty circle” property: the circumcircle of each triangle does not contain any other points. It is in some sense the most natural way to triangulate a set of points. We give below a general definition based on simplicial complexes.

Definition 1 Given a set $S \subset \mathbb{R}^n$ in general position, the *Delaunay Triangulation* of S is the simplicial complex $\text{DT}(S)$ consisting only of

1. all k -simplices, σ_T ($0 \leq k \leq n$), with $T \subset S$ such that the circumsphere (the smallest sphere such that all points lie on its boundary) of T does not contain any other points of S , and
2. all k -simplices which are faces of other simplices in $\text{DT}(S)$.

2.3. Alpha Complexes and Alpha Shapes

Alpha complexes are simplicial complexes that describe the levels of detail of a point set. By varying a positive real parameter α we obtain different shapes ranging from fine to crude. The most fine shape is the set of points, which is obtained when $\alpha = 0$. As α increases, the shape grows by adding simplices and develops cavities that may join to form tunnels and voids. The most crude shape is the Delaunay triangulation which is obtained for large values of α . More precisely, we have for alpha complexes the following definition:

Definition 2 Let $S \subset \mathbb{R}^n$ be a set of points in general position. For $T \subset S$ with $\#T \leq n$, let b_T and μ_T denote the smallest ball that contains the points of T and its radius, respectively. Given $0 \leq \alpha \leq \infty$, the α -complex $\mathcal{C}_\alpha(S)$ of S is the following simplicial subcomplex of $\text{DT}(S)$ where a simplex $\sigma_T \in \text{DT}(S)$ is in $\mathcal{C}_\alpha(S)$ if

1. $\mu_T < \alpha$ and $b_T \cap S = \emptyset$, or
2. σ_T is a face of another simplex in $\mathcal{C}_\alpha(S)$.

Looking at Delaunay triangulation and alpha complex definitions it is immediate the following properties:

- P1. If $\alpha_1 \leq \alpha_2$ then $\mathcal{C}_{\alpha_1} \subset \mathcal{C}_{\alpha_2}$,
- P2. $\mathcal{C}_\alpha \subset \text{DT}(S)$ and
- P3. $\mathcal{C}_\infty = \text{DT}(S)$.

The alpha shapes S_α is defined as the underlying polyhedron of an alpha complex $\mathcal{C}_\alpha(S)$, i. e., $S_\alpha = |\mathcal{C}_\alpha(S)|$. As well in the alpha complexes for large values of parameter α we obtain the Delaunay triangulation likewise in the alpha shapes we obtain precisely the convex hull. Indeed, an alpha shape is a suitable generalization of the convex hull concept that is used in several applications [7].

In this paper we are interested in the alpha complexes family because they are more appropriate to describe the combinatorial structure of an advancing front triangulation as well as its levels of detail. However, the alpha complex definition allows undesired simplices (dangling simplices)

of lower dimensions. Thus, it can't be considered a triangulation of a set of points. To accommodate this definition to triangulations, in the next subsection, we introduce a special version of the alpha complex: *the solid alpha-complex*.

2.4. Alpha Solid and Solid Alpha Complex

In general, the alpha-complexes and alpha shapes are mixed-dimension complexes and polytopes, respectively. Bernardini et al. [2] defined the *solid alpha-shapes* (or alpha-solid) as the alpha-shape without dangling and isolated k -simplices, $0 \leq k \leq n - 1$. In a similar way we define the *solid alpha complex* as the alpha complex without dangling and isolated k -simplices, $0 \leq k \leq n - 1$. It is a kind of a "regularized" subcomplex version of the alpha complex $\mathcal{C}_\alpha(\mathcal{S})$. In figure 1 we show a visual difference between alpha-complex and solid alpha complex, in the 2D case. The notation for the solid alpha-complex of $S \subset \mathbb{R}^n$, given $0 \leq \alpha \leq \infty$, is $\hat{\mathcal{C}}_\alpha(S)$.

Notice that the properties P1, P2 and P3 are still valid for the solid alpha complexes. This observation will be very important in section 6.

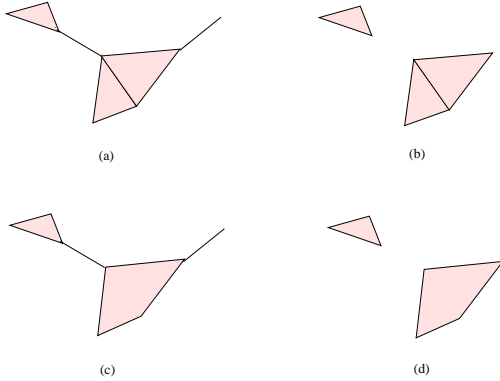


Figure 1. the alpha complex (a) and its solid alpha complex (b). The alpha shape (c) and its alpha solid (d).

3. The RBPA method

First, we will review the BPA, its main principles and data structure involved. In the sequence, we introduce our method, the RBPA, describing its natural inheritance from BPA and simplifications.

3.1. BPA review

The Ball-Pivoting Algorithm is an advancing front [10, 9] algorithm for surface reconstruction, one of the

most powerful among the incremental surface reconstruction methods. BPA is based on growing a surface by moving its boundary curves until the geometry and topology of the whole object is captured. For algorithms of this class it is necessary a criteria to choose a new element to be assigned to the mesh [11]. In the case of BPA, the criteria is a ball of fixed radius traversing the sample points by pivoting front edges of a current active boundary. Next, we summarize the geometric step, data structure involved and the mesh construction (algorithm outline). For more details [3, 11].

Geometric step. The input of the algorithm are three dimensional set points $P = \{p_1, p_2, \dots, p_n\}$, their normals and a fixed positive real parameter α . The geometric step of BPA takes a boundary edge $e_{ij} = \{p_i, p_j\}$ (pivot) and the sphere S of fixed radius α which has e_{ij} as a chord. The ball is turned around e_{ij} until it touches a point p_k . This point will be the only candidate to compose a new triangle with p_i and p_j (see Figure 2). For this candidate edge a test for normal consistence is performed and non-manifold cases are verified. To start the mesh construction there is another geometric routine, that find the seed triangle, i.e, three points such that the simplex they compose is not in the current mesh and it is α -exposed.

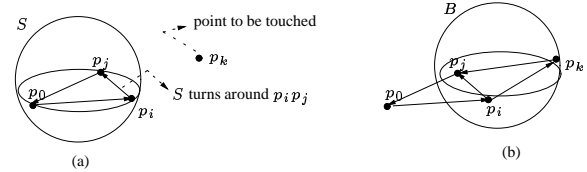


Figure 2. Ball Pivoting intuition. In the beginning the front is composed by the polygonal $p_1 p_2 p_3$ (a). After pivoting the new polygonal of the front is $p_1 p_2 p_3 p_4$ (b).

From the above description of the algorithm we have the following remark:

Observation 1 *The point p_k returned by the geometric step is such that $\sigma_T, T = \{p_k, p_i, p_j\}$, is α -exposed.*

Data structure. In general, BPA implementations have a graph G which represents point connectivity and two more fundamental data structures (e.g. half edge [1]). The first one is the front F , a collection of connected boundary curves that stores the contour of the current mesh front. The second fundamental data structure is a uniform 3D grid that takes advantage of the local property of the geometric step to speed up the algorithm. We define the size of the voxel in this grid as 2α . The reason for that is: a candidate to be

the first touched point is the one whose distance from it to the center of the pivoting chord is less than 2α . Notice that the grid takes linear time to be constructed. We will call the 27 neighbors voxels of a point p in the grid as V_p and denote $\#V_p$ as the number of points in V_p .

Algorithm outline. Initially the graph G contains only the first seed triangle and the front F corresponds to its three edges. The algorithm goes updating G by performing ball pivoting steps (candidate points are searched in V_p) once in each edge of the current front F until there is no more seed triangles. In each pivoting step this collection is updated by performing glue operations that join or separate boundary curves (for more details [11]).

3.2. Our method

Though BPA algorithm be usefull for 3D models, in general for range scans, we want to investigate what happen when we apply it in a set points restricted to a plane. More precisely, take an isometric embedding application $i : \mathbb{R}^2 \hookrightarrow \mathbb{R}^3$, say $i(x, y) = (x, y, 0)$ and apply BPA. This is what we call RBPA, a particular case of the BPA. We are now to discuss some particular features of RBPA which simplifies its implimentation, when compared to BPA:

- it use a 2D uniform grid: the neighbors of a point are on the 9 pixels around it instead of the 27 voxels of the 3D grid;
- there is neither normals consistence test (normals information is not necessary) nor non-manifold cases verification for candidate triangles;
- it is not necessary to treat the glue case when two boundary curves in the same connected component are joined into one (i. e., a genus could not be created in a planar surface); and
- the geometric step is simplified observing that to compute the smallest pivoting angle of the ball on some edge e_{ij} is equivalent to compute the biggest angle composed by the candidate point with e_{ij} (see fig. 3).

In its essence RBPA does not differ from BPA (note that observation 1 is also valid for RBPA). However, we are interested in its output and how it can contribute to 2D triangulation problems and sampling analysis in a qualitative and practical way. In the next section we show the RBPA relation with 2D solid alpha-complex.

4. 2D Solid Alpha-Complexes and RBPA

Now, we go to an important point of this paper by asking the following question:

How does the triangulation of RBPA look like, given $0 \leq \alpha \leq \infty$?

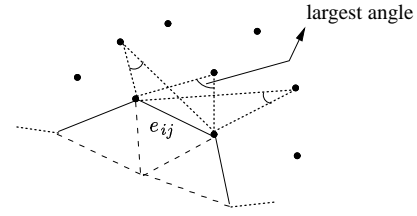


Figure 3. Geometric simplification of the candidate point selection.

The answer is: it looks like exactly to the 2D solid alpha-complex of the points. Indeed, let \mathcal{T}_α be the set of triangular faces built by RBPA. From observation 1 we have that each $\sigma_T \in \mathcal{T}_\alpha$ is α -exposed by a 3D-ball. Therefore, in the restricted plane its circumscribed circle b_T with radius μ_T is empty with $\mu_T \leq \alpha$. So, by definition 2, we have that $\mathcal{T}_\alpha \subset \hat{\mathcal{C}}_\alpha(S)$. To prove the converse we must suppose that the seed triangle selection is *ideal* in a sense that it returns a simplex iff there exists a set of three points $T = \{p_1, p_2, p_3\}$ such that σ_T is α -exposed and there is no segment of this triangle in the mesh. Let $\sigma_T \in \hat{\mathcal{C}}_\alpha(S)$. Since the seed selection is ideal, one segment of T , say p_1p_2 belongs to the mesh. At some moment running the RBPA, the segment p_1p_2 was in the front and one of the two cases could occur: (i) a pivoting was performed on p_1p_2 or (ii) it was glued to another boundary edge. Clearly, in the second case we have got to the conclusion. Since $\mu_T \leq \alpha$, in the first case p_3 is V_m , where m is the mid point of p_1p_2 , and geometrically it is the unique candidate point to be returned by the ball pivoting step. As a conclusion, in both cases we have $\sigma_T \in \hat{\mathcal{C}}_\alpha(S)$. More precisely, we have the following theorem:

Theorem 1 *Let $S \subset \mathbb{R}^2$ be a set of points in general position and $\hat{\mathcal{C}}_\alpha(S)$ its solid alpha-complex. Consider \mathcal{T}_α as the triangulation output of the RBPA running on the image of the embedding i with the “ideal” seed triangle selection. Then $\hat{\mathcal{C}}_\alpha(S) = \mathcal{T}_\alpha$.*

Note: Though in our implementation we do not have an “ideal” seed selection, to speed up the algorithm we adopted an heuristic that takes linear time independent on the number of calls. The approach looks at each pixel grid once and search for candidate triangles in a constant time. As we have a linear non empty number of pixels the total seed selection cost is linear.

Theorem 1 give us an important insight: it generates the 2D solid alpha complex without the computation of Delaunay triangulation. In the next section we will show that this computation is very efficient if, considering a suitable radius, we apply RBPA on uniform samplings. Indeed it has linear behaviour.

5. RBPA and uniform samplings

It is well-known that scan images generated by the points capture of object surfaces in 3D photography are very dense and are huge. This implies that surface reconstruction methods [12] should be efficient in order to deal with such type of data. The BPA uses a uniform 3D grid to accelerate the search. This strategy is very suitable because, in each ball pivoting step, only the points on the neighborhood V_p of the rotation center p are candidates to build a new triangle in the mesh. Moreover, if the object is uniformly sampled and the value of α is the less possible in such a way that the entire surface is reconstructed, then $\#V_p$ is very small and practically constant at any point of the surface. That is the reason why the BPA is very fast: the querying time at each pivoting step is constant and small. In other words, we can affirm that an optimal performance of the algorithm is achieved when such conditions of sampling characterize an “ideal” instance and the parameter α is sufficiently small. The same situation holds for RBPA.

We observe two disadvantages of the BPA, also present in the RBPA. When α is big, then $\#V_p$ is also big. Thus, at each pivoting step the algorithm spend more time searching for candidates in V_p . As a consequence, the algorithm slowdown at a point that is inneficient for large quantity of points. The other disadvantage occurs when the sampling is non-uniform. Beyond the same side effect cited above on uniform samplings, the values of $\#V_p$ are unbalanced at several regions. This fact also makes the algorithm inefficient.

In order to solve those problems, we are to propose a new methodology that accelerates the RBPA, iteratively running it with different radius in increasing scales of samplings (in our case we use the diadic scale) until we get to a desired radius. This new method will be denoted by HRBPA (Hierarchical RBPA). It calls RBPA several times in an adaptive way using the most suitable radius for the different sampling scales of the set of points. Moreover, it takes the advantage of the property that the complex generated at a iteration is enclosed on the complex of the previous iteration (property P1 in section 2.3). This allows us to eliminate points that are already on the interior of the mesh. Next section presents this method in detail.

6. HRBPA: Hierarchical RBPA

As we presented in the last section, HRBPA is in some sense a “multiscale” version of RBPA. This method speeds up the RBPA itself to compute solid alpha complexes given any positive real α and a generic sampling.

The methodology of HRBPA exploits the efficiency of RBPA with a suitable radius on uniform samplings combined with the solid alpha complex property that if $\alpha_1 \leq \alpha_2$

then $\hat{C}_{\alpha_1} \subset \hat{C}_{\alpha_2}$. More precisely, it applies iteratively RBPA in an adaptative way with a diadic resolution, i.e., from a “minimal” radius estimation α_0 in each interaction step, say i , we run RBPA with ball radius $2^i\alpha_0$. The total number of steps is $\log(\alpha/\alpha_0) + 1$. Next we explain how to estimate the minimal radius and how the iterative triangulation goes from one level step to the next one. Consider as input of HRBPA the real positive parameter α and the set of points S .

Minimal Radius Estimation. We tackled it by looking for small clusters of k -points in a quadtree constructed on the set of points such that each leaf has at most k points, where k is an integer controlled by the user. Then, we set α_0 as a half of the smallest leaf resolution (see fig 4.).

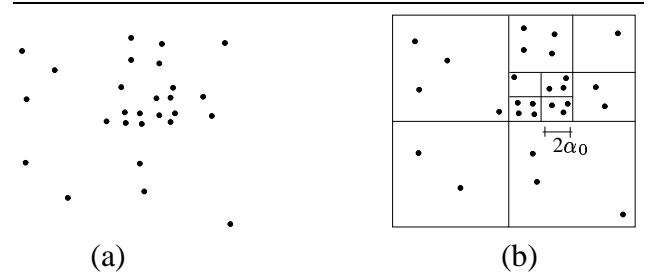


Figure 4. Computing the minimal radius resolution.

Iterative Triangulation After the minimal radius α_0 be estimated we evaluate $\alpha < 2\alpha_0$ (*). If (*) is true we apply RBPA with radius α and stop triangulation. Since $\hat{C}_{\alpha_0} \subset \hat{C}_{2\alpha_0}$, in the case of (*) be false, we apply again RBPA with radius $2\alpha_0$ only on the points lying in the set $S - \text{int}(\hat{C}_{\alpha_0})$ by advancing the boundary of \hat{C}_{α_0} , which composes the front F . Therefore, to go from a lower to the higher resolution, we need only transfer boundary and isolated points (see fig. 5) and continue advancing the front F . Analogously, we apply the same process to the others levels.

Summarizing HRBPA, for $0 \leq \alpha \leq \infty$ we have the following steps:

1. Compute minimal radius α_0 , set $\alpha_i = \alpha_0$ and $i = 0$;
2. Transfer boundary and isolated points as input;
3. If $\alpha < \alpha_i$ then apply RBPA with radius α and stop, else apply it with radius α_i ;
4. Set $i = i + 1$, $\alpha_i = 2\alpha_{i-1}$ and go back to step 2.

Complexity. The HRBPA complexity for $\alpha = \alpha_0$, without considering the complexity of the quadtree construction,

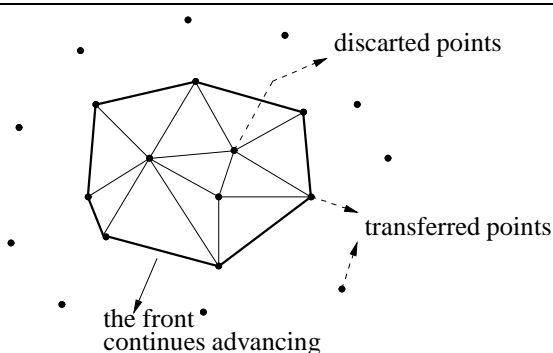


Figure 5. Iterative triangulation step.

corresponds to the “ideal” RBPA case on regular samplings and it has linear behaviour because in each pivoting step we have that $\#V_p$ is constant. Most part of the linear constant depends on data structure implementation¹ and on the parameter k as the maximum number of points in each leaf. In figure 6 we show a graphic to illustrate RBPA linearity on uniform samplings.

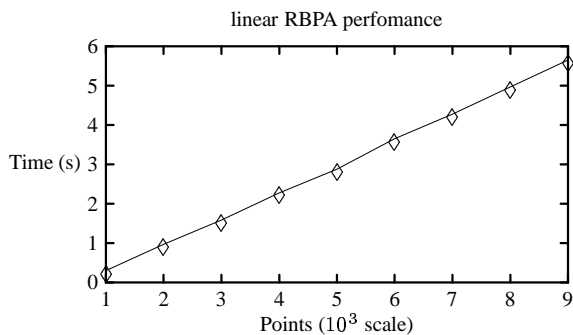


Figure 6. Timing graphic.

For generic samplings we do not have a global complexity bound on the number of points but we can analyse and evaluate it in parts.

The preprocessing cost to build the quadtree depends on the depth d of the quadtree which can be shown that $d = \log(s/c) + 3/2$ where s is the side length of the initial square and c is the diameter of the smallest cluster with k points (adaptated from [5] cap 14 pg. 293). Therefore building the quadtree takes $O((d+1)n)$ time, where n is the number of points.

¹ We used a generic data structure [14] which comprises geometry and topology in a unified framework for representations of meshes with or without boundaries. It is a very flexible framework that makes easier future advanced studies on topology and sampling analyses we plan as a future work.

There is also the triangulation cost in each iteration step considering only the boundary and isolated points of the previous triangulation step to continue advancing the front. Since at each level we apply RBPA with the appropriate radius (i. e. we fall in the ideal case of RBPA) thus we have a linear bound time. In conclusion, if there are k_i boundary and isolated points in the level step i , RBPA takes $O(k_i)$ time cost to transfer these points, build the grid data structure and perform triangulation. Therefore the total cost of HRBPA is $O((d+1)n + \sum k_i)$, where $k_j \leq k_i$ for $i < j$.

7. Examples

In figures 7, 8 and 9 we summarize applications with examples.

Figure 7 shows in the first picture a uniform sampling of the alpha symbol and its quadtree structure detecting a minimal resolution of the points. Applying HBPA in the ideal case ($\alpha = \alpha_0$), we obtain a nice result by recovering the actual shape of the samples. As we depicted in (a) and (b) the recognized shape can be represented through the solid alpha complex or through its alpha solid, respectively.

Figure 8 shows an example which is very applicable to computational biology analysis and related domains. In picture (a) we have a preprocessed image of a molecule and its quadtree structure detecting minimal resolution. Running HRBA with the minimal radius it did not capture the whole topology (i.e. atoms) of the molecule (see picture (b)). However, by increasing slightly the radius we obtain the correct one (see picture (c)).

In figure 9 we show an example that illustrate how HBPA improves RBPA performance. In the first picture we have a non uniform sampling containing 700 points and its two resolution levels (α_0 and $2\alpha_0$) captured by the quadtree structure. Applying RBPA with radius size in the largest level ($\alpha = 2\alpha_0$) we obtain, as a result, the alpha complex depicted in (c) at time running of 50ms. Applying HRBPA, which first compute the alpha complex depicted in (b), we obtain for the same radius the time running of 25ms (more precisely 15ms in the first level and 8ms in the second one).

8. Conclusion

Based on BPA principles, in this paper we introduced the concept of *solid alpha complexes*. We present a new method for the construction of this kind of object, the RBPA. We showed that RBPA is an algorithm whose efficiency is dependent on the uniformity of the sample points and on the ball size. To solve this problem we proposed the hierarchical RBPA (HRBPA), which generalizes the RBPA method. It obtains, in an adaptive way, 2D solid alpha complexes of generic samplings (uniform or non-uniform) free from the influence of ball size.

Future Work

At small term we are chasing two main results:

- Generalize RBPA for 3D points to compute tetrahedralizations,
- Take advantage of the quadtree as query structure instead of a uniform grid. This avoids HRBPA creating uniform grid at each level.

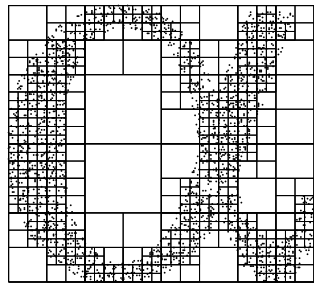
We are also to investigate applications to geometric and topological sampling analysis.

Acknowledgements

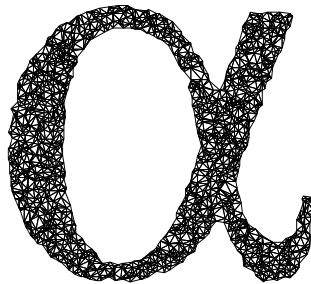
This research has been developed in the VISGRAF Laboratory at IMPA with. VISGRAF is sponsored by CNPq, FAPERJ, FINEP and IBM Brasil.

References

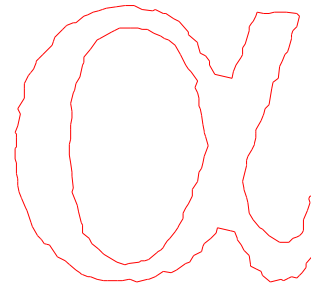
- [1] B. Baumgart. A polyhedron representation for computer vision. *AFIPS Conf. Proc.*, pages 589–596, 1975.
- [2] F. Bernardini, C. L. Bajaj, J. Chen, and D. R. Schikore. Automatic reconstruction of 3d cad models from digital scans. *Int. J. on Comp. Geom. and Appl.*, 9(4-5):327–369, 1999.
- [3] F. Bernardini, J. Mittleman, H. Rushmeir, and C. Silva. The ball-pivoting algorithm for surface reconstruction. *IEEE Trans. Visual. Comput. Graphics*, 5(8):349–359, 1999.
- [4] F. Bernardini and H. Rushmeier. The 3d model acquisition pipeline. *Computer Graphics forum*, 21(2):149–172, 2002.
- [5] M. de Berg, O. Schwarzkopf, M. van Kreveld, and M. Overmars. *Computational geometry: algorithms and applications*. Springer-Verlag, 2nd rev. ed. 2000.
- [6] H. Edelsbrunner, D. G. KirkPatrick, and R. Seidel. On the shape of a set of points in the plane. *IEEE Trans. Inform. Theory*, 29:521–559, 1983.
- [7] H. Edelsbrunner and E. P. Mucke. Three-dimensional alpha shapes. *ACM Trans. Graph.*, 10(1):43–72, 1994.
- [8] S. Fortune. Voronoi diagrams and delaunay triangulations. *Computing in Euclidean Geometry (Lecture Notes Series on Computing)*, 1:193–233, 1992.
- [9] P. George and E. Seveno. The advancing front mesh generation method revisited. *International Journal for Numerical Methods in Engineering*, 37:3605–3619, 1994.
- [10] S. H. Lo. A new mesh generation scheme for arbitrary planar domains. *International Journal for Numerical Methods in Engineering*, 21:1403–1426, 1985.
- [11] E. Medeiros. A topological framework for advancing front triangulations. *Proceedings of the XVI Brazilian Symposium on Computer Graphics and Image Processing, IEEE Press*, pages 45–51, 2003.
- [12] E. Mencl and H. Muller. Interpolation and approximation of surfaces from three-dimensional scattered data points. *ACM Eurographics 98 (State of the Art Reports)*, pages 63–69, 1998.
- [13] P. Su and R. L. S. Drysdale. A comparison of sequential delaunay triangulation algorithms. *Proc. 11th Annual Symp. on Comp. Geo.*, 1:61–70, June 1995.
- [14] L. Velho, H. Lopes, and G. Tavares. Mesh ops. *preprint*.



(a)

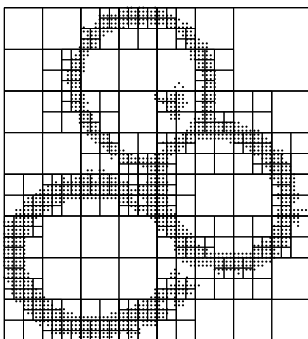


(b)

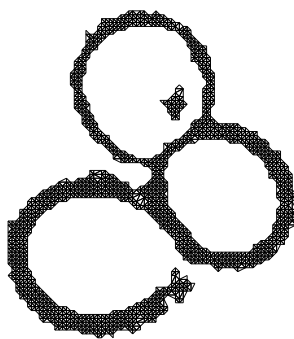


(c)

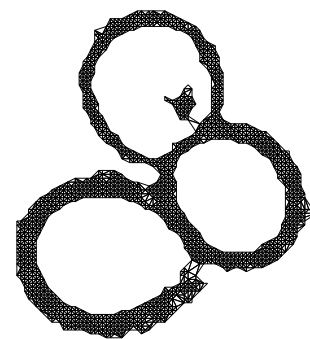
Figure 7. (a) sampling of the alpha symbol, its (b) solid alpha complex and its (c) alpha solid.



(a)

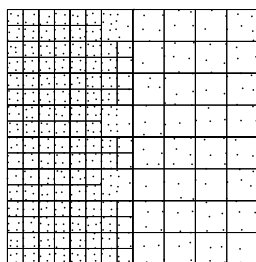


(b)

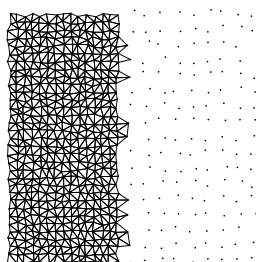


(c)

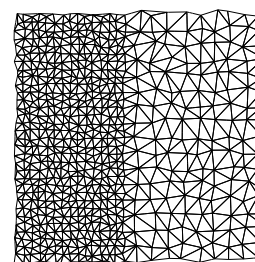
Figure 8. Preprocessed image of a molecule (a), its solid alpha complex for $\alpha = \alpha_0$ (b) and its topology recovered with a slight increase in the ball size (c).



(a)



(b)



(c)

Figure 9. Multiscale sampling with two levels (a) and two reconstructed levels of detail, (b) and (c).